Contribution from the CNR, Centro di Studio per la Sintesi e la Struttura dei Composti dei Metalli di Transizione nei Bassi Stati di Ossidazione and Dipartimento di Chimica Inorganica e Metallorganica, Via G. Venezian 21, 20133 Milano, Italy, Istituto di Chimica Farmaceutica, Università di Milano, Viale Abruzzi 42, 20133 Milano, Italy, and Dipartimento di Chimica del Politecnico di Milano, Piazza L. Da Vinci 32, 20133 Milano, Italy

Mixed Platinum–Rhodium Carbonyl Clusters. Synthesis and Chemical Characterization of the $[PtRh_6(\mu_3\text{-}CO)_3(\mu\text{-}CO)_5(CO)_8]^{2-}$ Anion and X-ray Crystal Structure of Its Tetrapropylammonium Salt†

Alessandro Fumagalli,*[1a] Secondo Martinengo,[1a] Daniele Galli,[1a] Alberto Albinati,*[1b] and Fabio Ganazzoli[1c]

Received November 11, 1988

The dianion $[PtRh_6(CO)_{16}]^{2-}$ has been obtained through several synthetic routes, particularly by redox condensation of $[PtRh_5(CO)_{15}]^-$ and $[Rh(CO)_4]^-$. The product is unstable in solution, both under N_2, where it slowly yields species of higher nuclearity, and under CO, where it is fragmented in smaller clusters. The $[N\text{-}n\text{-}Pr_4]_2[PtRh_6(CO)_{16}]$ salt has been characterized by X-ray diffraction. Crystal data: $C_{40}H_{56}N_2O_{16}PtRh_6$, M_r = 1633.41, monoclinic, space group $C2/c$ (No. 15), a = 17.180 (2) Å, b = 15.848 (2) Å, c = 39.719 (4) Å, β = 92.45 (3)°, Z = 8, R = 0.048, R_w = 0.063. The metal skeleton of the dianion is an octahedron of Rh atoms asymmetrically capped by a Pt atom. Three carbonyls out of 16 are triply bridging, five are edge bridging, and eight are terminal (two on a Rh atom of the capped face and one on each of the other metals). One of the two terminal carbonyls bound to the unique rhodium is heavily distorted (Rh–C–O = 158 (3)°) by a weak semibridging interaction with the Pt atom (Pt···C = 2.73 (3) Å).

Introduction

We have reported so far several Pt–Rh carbonyl cluster anions: three low-nuclearity species ($[PtRh_5(CO)_{15}]^-$,[2] $[PtRh_4(CO)_{14}]^{2-}$,[2] and $[PtRh_4(CO)_{12}]^{2-}$[2]) and a few others, derived from these three, with a nuclearity ranging from 11 up to 22 ($[Pt_2Rh_9(CO)_{22}]^{3-}$,[3] $[PtRh_{12}(CO)_{24}]^{4-}$,[4] $[Pt_2Rh_{11}(CO)_{24}]^{3-}$,[4] and $[Pt_4Rh_{18}(CO)_{35}]^{4-}$[5]). More recently, we have focused our interest toward those species of intermediate nuclearity that are generally characterized by a high reactivity, in that they show tendency to evolve in either direction, toward the lower or higher nuclearities. A first result in this study was the synthesis of $[PtRh_8(CO)_{19}]^{2-}$.[6] The investigation leading to the isolation of another species of this class, the presently reported $[PtRh_6(CO)_{16}]^{2-}$, originated from the hypothesis that, due to the existence of $[NiRh_6(CO)_{16}]^{2-}$,[7] an analogous Pt–Rh cluster could also exist. We therefore searched for synthetic methods that could afford this species, investigating various possible routes, including redox condensations, direct synthesis from Rh(III) and Pt(IV) salts, and reduction of $[PtRh_5(CO)_{15}]^-$ under nitrogen.

Results

1. Synthesis of $[PtRh_6(CO)_{16}]^{2-}$. The first attempt to synthesize the $[PtRh_6(CO)_{16}]^{2-}$ anion was done by the redox condensation

$$[PtRh_4(CO)_{14}]^{2-} + \tfrac{1}{2}Rh_4(CO)_{12} \rightarrow [PtRh_6(CO)_{16}]^{2-} + 4CO \quad (1)$$

The reaction was carried out in acetone or tetrahydrofuran (THF) under nitrogen at room temperature with the $[PPN]^+$[8] or the $[N\text{-}n\text{-}Bu_4]^+$ salts of $[PtRh_4(CO)_{14}]^{2-}$.[2] Close IR monitoring indicated a complex reaction path, consisting of several intermediate steps, yielding in a few hours a brown, sometimes greenish, mixture of several species. The green main product, isolated by fractional precipitation, showed an IR spectrum closely similar to that of $[NiRh_6(CO)_{16}]^{2-}$, thus suggesting that it could very likely be the corresponding Pt derivative. However, the low yields induced us to search for other syntheses, and in fact we found that the green dianion can be obtained more conveniently by the redox condensation of $[PtRh_5(CO)_{15}]^-$[2] with $[Rh(CO)_4]^-$[9] in a 1:1 molar ratio:

$$[PtRh_5(CO)_{15}]^- + [Rh(CO)_4]^- \rightarrow [PtRh_6(CO)_{16}]^{2-} + 3CO \quad (2)$$

The reaction proceeds quickly and results in the desired condensation (2), with yields up to 80%, when the solvent is THF and the countercation is $[PPN]^+$. In this same solvent, if the sodium salts are used, there is instead a redox reaction, yielding $[Rh_6(CO)_{15}]^{2-}$,[10] $[Rh_7(CO)_{16}]^{3-}$,[10] and an unknown brown species. This suggests a strong ionic coupling influence, which is confirmed by the fact that when the solvent is changed to methanol or acetone the reaction of the sodium salts also gives good yields. Reaction 2 is particularly useful because it makes it possible to obtain by metathesis from $Na_2[PtRh_6(CO)_{16}]$ several crystalline derivatives with different bulky cations, such as $[PPN]^+$, $[PPh_4]^+$, and $[N\text{-}n\text{-}Pr_4]^+$. Only the last of these derivatives was found suitable for the X-ray structural analysis (see below).

An attempt to directly synthesize $[PtRh_6(CO)_{16}]^{2-}$ was done by taking Na_2PtCl_6 and $RhCl_3{\cdot}xH_2O$ in the correct 1:6 ratio and submitting the mixture to reductive carbonylation in methanol under CO, with use of such an amount of NaOH to reach, at the end of the carbonylation, a reduction state intermediate between those of $[PtRh_5(CO)_{15}]^-$ and $[PtRh_4(CO)_{14}]^{2-}$. The IR spectra showed that, under these conditions, some $[Rh_5(CO)_{15}]^-$[11] is also formed. The mixture, upon CO evacuation, gave some $[PtRh_6(CO)_{16}]^{2-}$, but in low yields, making this reaction not convenient.

In a previous work we reported that $[PtRh_5(CO)_{15}]^-$ is easily reduced under CO with loss of one rhodium atom and formation of $[PtRh_4(CO)_{14}]^{2-}$,[2] with no evidence of other intermediate mixed species. This was rather surprising because, due to the large difference in the ratio (negative charge): (number of metal atoms) between the reactant and the product, i.e., 1:6 and 2:5, respectively, some intermediate species were expected. As the absence of such

† Taken in part from: Galli, D. Thesis, Università di Milano.

(1) (a) Centro CNR and Dipartimento di Chimica Inorganica e Metallorganica. (b) Università di Milano. (c) Politecnico di Milano.
(2) (a) Fumagalli, A.; Martinengo, S.; Chini, P.; Albinati, A.; Bruckner, S.; Heaton, B. T. *J. Chem. Soc., Chem. Commun.* **1978**, 195. (b) Fumagalli, A.; Martinengo, S.; Chini, P.; Galli, D.; Heaton, B. T.; Della Pergola, R. *Inorg. Chem.* **1984**, *23*, 2947.
(3) Fumagalli, A.; Martinengo, S.; Ciani, G. *J. Organomet. Chem.* **1984**, *273*, C46.
(4) Fumagalli, A.; Martinengo, S.; Ciani, G. *J. Chem. Soc., Chem. Commun.* **1983**, 1381.
(5) Fumagalli, A.; Martinengo, S.; Ciani, G.; Masciocchi, N.; Sironi, A. Presented at the XVIII National Congress on Inorganic Chemistry, Como, Italy, 1985; Abstract No. A30.
(6) Fumagalli, A.; Martinengo, S.; Ciani, G.; Marturano, G. *Inorg. Chem.* **1986**, *25*, 592.
(7) (a) Fumagalli, A.; Longoni, G.; Chini, P.; Albinati, A.; Bruckner, S. *J. Organomet. Chem.* **1980**, *202*, 329. (b) Heaton, B. T.; Della Pergola, R.; Strona, L.; Smith, D. O.; Fumagalli, A. *J. Chem. Soc., Dalton Trans.* **1982**, 2553.
(8) $[PPN]^+$ = bis(triphenylphosphine)nitrogen(1+) cation.
(9) (a) Chini, P.; Martinengo, S. *Inorg. Chim. Acta* **1969**, *3*, 21. (b) Garlaschelli, L.; Chini, P.; Martinengo, S. *Gazz. Chim. Ital.* **1982**, *112*, 285.
(10) Martinengo, S.; Chini, P. *Gazz. Chim. Ital.* **1972**, *102*, 344.
(11) Fumagalli, A.; Koetzle, T. F.; Takusagawa, F.; Chini, P.; Martinengo, S.; Heaton, B. T. *J. Am. Chem. Soc.* **1980**, *102*, 1740.

0020-1669/89/1328-2476$01.50/0

species could be due to the presence of CO, we decided to investigate the reduction of $[PtRh_5(CO)_{15}]^-$ under nitrogen.

A first rough screening of various reducing systems indicated that the reduction path under nitrogen is indeed more complex than under CO, and mixtures of higher nuclearity clusters are eventually obtained. The composition of these mixtures was found reproducible with difficulty because it is dependent upon the particular reducing agent, its addition rate, and the reaction time. However, a close IR monitoring of the reaction course indicated that in all the investigated systems $[PtRh_6(CO)_{16}]^{2-}$ appeared as a transient species in the early stages of the reductive sequence; this suggested that mild reducing systems would be more convenient for its isolation. Thus, a series of experiments was done by treating $Na[PtRh_5(CO)_{15}]$ in methanol with excess Na_2CO_3, which, due to its low solubility, gives a slow reaction that can be stopped at any point by filtration of the carbonate. Under these conditions we found that the highest concentration of the product is reached when a greenish brown solution is formed, whose IR spectrum shows broad bands centered at ca. 2000 and 1790 cm^{-1} in the terminal and bridging CO stretching regions, respectively. Addition of bulky cation salts to this solution causes precipitation of a mixture of products from which the green $[PtRh_6(CO)_{16}]^{2-}$ anion can be isolated by extraction with THF and fractional crystallization. If the reaction is not stopped at this point, the $[PtRh_6(CO)_{16}]^{2-}$ anion slowly disappears, as indicated by a progressive shift of the bridging CO band toward slightly higher wavenumbers. This is related to the formation of species of higher nuclearity, which generally bear doubly rather than triply bridging carbonyls; one of these species was in fact recognized as $[Pt_2Rh_{11}(CO)_{24}]^{3-}$.[4] The difficulty in establishing the optimum end point of the reaction and the care required in subsequent manipulations make this method not convenient with respect to the above cited redox condensation (2).

2. Characterization of $[PtRh_6(CO)_{16}]^{2-}$. All the products obtained with different cations were generally stable in the air for a few hours in the solid state but decomposed within minutes in solution. In any case $[PtRh_6(CO)_{16}]^{2-}$ in solution appears as a rather unstable species even under nitrogen and gives slow decomposition, yielding other as yet uncharacterized species. This decomposition becomes evident when crystals are grown by the slow diffusion of 2-propanol into THF solutions of the compound; due to the long diffusion time, one always obtains, along with some crystalline specimens, oily byproducts mostly insoluble in THF.

The green $[PtRh_6(CO)_{16}]^{2-}$ dianion reacts readily at room temperature with CO at atmospheric pressure, yielding orange-brown solutions containing $[Rh_5(CO)_{15}]^-$,[11] $[PtRh_4(CO)_{14}]^{2-}$, and $[PtRh_5(CO)_{15}]^-$. The three products were separated by fractional precipitation of the $[PPN]^+$ salts on stepwise addition of *n*-pentane and individually identified by their characteristic IR spectra. The stoichiometry of the reaction is apparently

$$3[PtRh_6(CO)_{16}]^{2-} + 10CO \rightarrow 2[PtRh_4(CO)_{14}]^{2-} + [Rh_5(CO)_{15}]^- + [PtRh_5(CO)_{15}]^- \quad (3)$$

This reaction explains the lack of formation of $[PtRh_6(CO)_{16}]^{2-}$ in the reduction of $[PtRh_5(CO)_{15}]^-$ under CO. Only partial reversibility is observed upon evacuation of CO, because of the formation, besides to $[PtRh_6(CO)_{16}]^{2-}$, of other brown unidentified products. This behavior explains the low yields obtained in the above-mentioned attempt to directly synthesize $[PtRh_6(CO)_{16}]^{2-}$ from Na_2PtCl_6 and $RhCl_3$, which in fact, prior to CO evacuation, yields a system quite similar to that of the right-hand side of eq 3.

3. IR Spectra of $[PtRh_6(CO)_{16}]^{2-}$. These spectra show some dependence on the cation, probably because of ion pairing; this effect is more pronounced in the bridging CO region, where the spectra of the other salts are slightly different, in both the shape and position of the bands, from that of the $[PPN]^+$ salt reported in Figure 1. For instance, in THF, the $[PPN]^+$ and $[N\text{-}n\text{-}Pr_4]^+$ salts have bands (±5 cm^{-1}) at 2032 w, 1989 vs, 1838 mw, 1824 mw, 1805 ms, and 1776 m and at 2020 w, 1990 vs, 1835 mw (br), 1800 m, and 1780 m (br), respectively. These spectra are very similar to those of the corresponding salts of $[NiRh_6(CO)_{16}]^{2-}$,

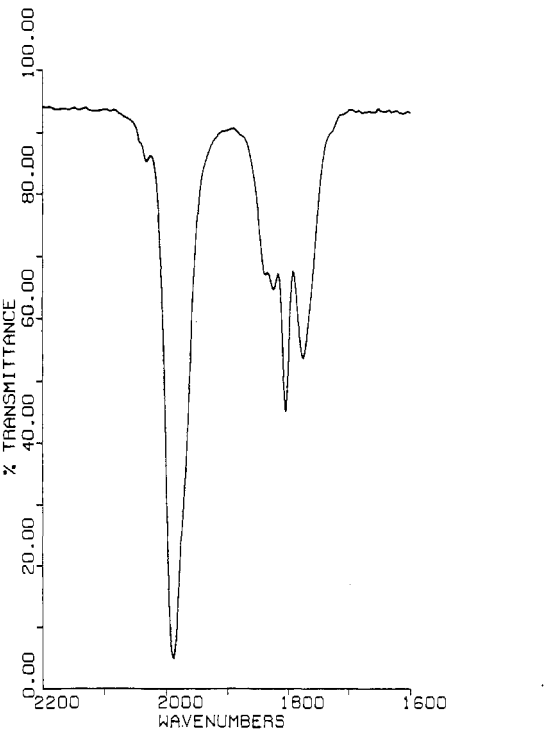

Figure 1. FT IR spectrum of $[PtRh_6(CO)_{16}]^{2-}$ as the $[PPN]^+$ salt in THF with solvent subtraction.

Table I. Relevant Distances (Å) in the Dianion $[PtRh_6(CO)_{16}]^{2-}$

		M–M	
Pt–Rh(1)	2.698 (2)	Rh(2)–Rh(6)	2.857 (3)
Pt–Rh(2)	3.167 (2)	Rh(3)–Rh(4)	2.746 (3)
Pt–Rh(6)	2.771 (2)	Rh(3)–Rh(5)	2.730 (3)
Rh(1)–Rh(2)	2.830 (3)	Rh(3)–Rh(6)	2.814 (3)
Rh(1)–Rh(4)	2.834 (3)	Rh(4)–Rh(5)	2.795 (3)
Rh(1)–Rh(5)	2.751 (3)	Rh(4)–Rh(6)	2.781 (3)
Rh(1)–Rh(6)	2.820 (3)	Rh(1)···Rh(3)	3.908 (3)
Rh(2)–Rh(3)	2.810 (3)	Rh(2)···Rh(4)	4.023 (3)
Rh(2)–Rh(5)	2.844 (3)	Rh(5)···Rh(6)	3.950 (3)
		M–C (Terminal)	
Pt–C(8)	1.77 (3)	Rh(3)–C(3)	1.82 (3)
Rh(1)–C(1)	1.84 (3)	Rh(4)–C(4)	1.92 (3)
Rh(2)–C(2)	1.88 (3)	Rh(5)–C(5)	1.85 (3)
Rh(2)–C(7)	1.90 (3)	Rh(6)–C(6)	1.86 (3)
		M–C (Double Bridge)	
Pt–C_b(1)	2.14 (3)	Rh(3)–C_b(3)	2.05 (3)
Pt–C_b(5)	2.12 (3)	Rh(4)–C_b(3)	2.00 (3)
Rh(1)–C_b(1)	1.98 (3)	Rh(4)–C_b(4)	1.98 (3)
Rh(3)–C_b(2)	2.05 (3)	Rh(5)–C_b(4)	2.01 (3)
Rh(5)–C_b(2)	2.00 (3)	Rh(6)–C_b(5)	1.97 (3)
		M–C (Triple Bridge)	
Rh(1)–C_t(1)	2.14 (3)	Rh(5)–C_t(2)	2.29 (3)
Rh(4)–C_t(1)	2.25 (3)	Rh(2)–C_t(3)	2.28 (3)
Rh(6)–C_t(1)	2.15 (2)	Rh(3)–C_t(3)	2.31 (3)
Rh(1)–C_t(2)	2.29 (3)	Rh(6)–C_t(3)	2.04 (3)
Rh(2)–C_t(2)	2.11 (3)		
		C–O[a]	
C_{term}–O	1.18 (3)	C_t–O	1.21 (4)
C_b–O	1.19 (3)		

[a] Average value; the standard deviation on the mean has been obtained from the formula $s = [\sum(d_i - \bar{d})^2/(n-1)]^{1/2}$.

as expected from the almost identical structural features (vide infra).

4. Structure of $[PtRh_6(CO)_{16}]^{2-}$. A perspective view of the anion is shown in Figure 2, while relevant bond lengths and angles are reported in Tables I and II.

Discussion of the Structure

The metal cluster is formed by a distorted octahedron of Rh atoms capped on a face by a Pt atom. The cluster geometry is

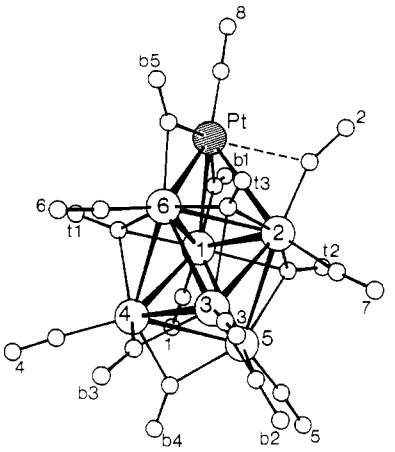

Figure 2. View of the anion $[PtRh_6(\mu_3\text{-}CO)_3(\mu\text{-}CO)_5(CO)_8]^{2-}$. The carbonyl ligands are indicated by the numbers of their oxygen atoms.

best discussed in comparison with the analogous $[NiRh_6(CO)_{16}]^{2-}$;[7] however, in the present case, the distortion of the Rh framework from the octahedral symmetry cannot be rationalized in simple terms, unlike that of the Ni–Rh compound, where a trigonal-antiprismatic distortion was easily detected. In fact, the Rh–Rh bond distances span the whole range from 2.730 (3) to 2.857 (3) Å; although some general trend may still be recognized, the differences in bond lengths between the metals belonging to different faces are only marginally significant ($\pm 2\sigma$).

With reference to Figure 2, the top triangular face defined by Rh(1), Rh(2), and Rh(6) and capped by the Pt atom shows the longest bond distances (average 2.836 (19) Å), whereas the bottom face, defined by atoms Rh(3), Rh(4), and Rh(5), shows the shortest separations (average 2.757 (34) Å). The average value of the six bond lengths between these faces, 2.806 (34) Å, falls in between, with such a distribution of the single values that the planes defined by the top and bottom faces are essentially parallel, forming a dihedral angle of 0.86 (7)°; this is at variance with what is found in $[NiRh_6(CO)_{16}]^{2-}$.

Moreover, the three lateral faces that are triply bridged by a carbonyl show Rh–Rh separations (average 2.82 Å) consistently larger than those found for the other lateral faces (average 2.79 Å). Although these differences are systematic for the two sets of distances, they are significant only at the 1σ level.

As found in other related compounds,[12,13] the capping Pt atom is asymmetrically bonded to the Rh atoms, showing two shorter (average 2.735 (2) Å) and one longer bond length (3.167 (2) Å), with one of the largest differences, 0.43 Å, reported thus far; as a result, the Pt atom is 0.58 Å off the idealized C_3 noncrystallographic axis of the Rh_6 octahedron. The shorter Pt–Rh bonds are bridged by two carbonyls with shorter Rh–C (average 1.978 (4) Å) and longer Pt–C bond lengths (average 2.128 (17) Å): this is consistent with the difference in covalent radii, though it is larger than expected. We also note that (i) the Pt...C(2) separation is short at 2.73 (3) Å and (ii) the Rh(2)–C(2)–O(2) bond angle has a value of 158 (3)°, which is approximately halfway between the average value of 176 (2)° for terminal carbonyls and that of 137 (3)° for the edge-bridging carbonyls. This is consistent with the C(2)–O(2) ligand being semibridging on the Pt–Rh(2) edge.

The other carbonyls are in the same arrangement found in $[Rh_7(CO)_{16}]^{3-}$ and $[NiRh_6(CO)_{16}]^{2-}$: each metal atom bears a terminal carbonyl and the three edges of the bottom face are spanned by three double-bridging carbonyls. Three of the six lateral faces, that is, [Rh(2), Rh(3), Rh(6)], [Rh(1), Rh(2), Rh(5)], and [Rh(1), Rh(4), Rh(6)] are triply bridged by carbonyls. The Rh–C bond distances have increasingly larger average values of 1.87 (4) Å for terminal CO, 2.01 (3) Å for double-bridging CO, and 2.21 (10) Å for triple-bridging CO.

The tetra-*n*-propylammonium cations have the expected geometry with average bond lengths of 1.56 (3) Å for C–N and 1.55 (3) Å for C–C.

Concluding Remarks

The anion $[PtRh_6(CO)_{16}]^{2-}$ is isoelectronic with most of the known monocapped octahedral species,[12] possessing 98 cluster valence electrons, in accord with various cluster electron-counting theories.[14]

This is a very reactive species, in that it easily decomposes under a nitrogen atmosphere, yielding higher nuclearity clusters. The reason for this instability is perhaps due to the presence of a formally electron-deficient Pt atom with a local environment very reminiscent of that found in the analogously reactive species $[PtRh_4(CO)_{12}]^{2-}$ and $[PtIr_4(CO)_{12}]^{2-}$;[13] this unsaturation would be the driving force to reach the higher metallic connectivity that is peculiar to platinum in the larger clusters.[3-6] It has also to be remarked that, with reference to the reaction (2), where a Rh atom condenses on the $PtRh_5$ octahedron, a nontrivial skeletal rearrangement is required to relocate the platinum from one vertex of the octahedral moiety to the capping position. Skeletal rearrangements of this kind have already been evidenced in bimetallic Pt–Rh and Pt–Ir clusters.[2,13]

Finally, it may be interesting to note that the reaction of $[PtRh_6(CO)_{16}]^{2-}$ with CO (eq 3) gives a fragmentation different from that of the analogous $[NiRh_6(CO)_{16}]^{2-}$,[7] which yields only two products, $[Rh_6(CO)_{15}]^{2-}$ and $Ni(CO)_4$, in a reversible equilibrium. This different behavior can be explained as a consequence of the M–CO vs M–M energy balance, which favors the $Ni(CO)_4$ formation, and of the greater bonding energy E_{Pt-Rh} in comparison with E_{Ni-Rh}, assuming E_{M-Rh} is about equal to $(E_{M-M} + E_{Rh-Rh})/2$.[15]

Experimental Section

All the reactions and subsequent manipulations were carried out under a nitrogen or carbon monoxide atmosphere in carefully purified solvents saturated with nitrogen. $Rh_4(CO)_{12}$[16] and $[PPN]^+$ or Na^+ salts of $[PtRh_4(CO)_{14}]^{2-}$,[2] $[PtRh_5(CO)_{15}]^-$,[2] and $[Rh(CO)_4]^-$[9] were prepared according to the literature. The solution of $Na[Rh(CO)_4]$ was prepared by reduction of $Rh_4(CO)_{12}$ with sodium metal in THF under CO and was analyzed for the exact rhodium content. Infrared spectra were recorded on Perkin-Elmer 457 and 297 grating spectrophotometers and on a Nicolet MX-1 FT IR instrument using 0.1 mm calcium fluoride cells previously purged with nitrogen or CO.

1. Synthesis of $[PtRh_6(CO)_{16}]^{2-}$. (a) From $[PtRh_4(CO)_{14}]^{2-}$ and $Rh_4(CO)_{12}$. $[PPN]_2[PtRh_4(CO)_{14}]$ (566 mg, 0.272 mmol) and $Rh_4(CO)_{12}$ (105 mg, 0.140 mmol) were dissolved under nitrogen in 10 mL of acetone. The solution was stirred and briefly evacuated twice, over a period of 5 h, in order to remove the evolved CO; the color turned from red to brown. Addition of 2-propanol (10 mL) caused precipitation of some black oily material, leaving a green solution. After the mixture stood overnight, the solution was separated from the insoluble material and evaporated to dryness under vacuum; redissolution in THF (5 mL) and slow diffusion of 2-propanol (20 mL) gave black crystals of the product together with some tacky material.

(b) From $[PPN][PtRh_5(CO)_{15}]$ and $[PPN][Rh(CO)_4]$. $[PPN][PtRh_5(CO)_{15}]$ (365 mg, 0.218 mmol, in 10 mL of THF) was treated with $[PPN][Rh(CO)_4]$ (10 mL of a 0.0218 M solution in THF). After the mixture was stirred for 2 h, the green solution was filtered and 2-propanol (50 mL) added with stirring. By concentration under vacuum, a microcrystalline green precipitate was obtained; the brown mother liquor was filtered off and the product washed with 2-propanol (2 × 10 mL) and vacuum-dried; yield 0.390 g (77%). Anal. Found (calcd) for $[PPN]_2[PtRh_6(CO)_{16}]$: C, 45.56 (45.21); H, 2.81 (2.59); N, 1.15 (1.20); Rh, 25.31 (26.41).

(c) From $Na[PtRh_5(CO)_{15}]$ and $Na[Rh(CO)_4]$. A THF solution of $Na[Rh(CO)_4]$ containing 0.33 mmol of the compound was almost vac-

(12) Albano, V. G.; Bellon, P. L.; Ciani, G. *J. Chem. Soc., Dalton Trans.* **1988**, 1103 and references therein.
(13) Fumagalli, A.; Della Pergola, R.; Bonacina, F.; Garlaschelli, L.; Moret, M.; Sironi, A. *J. Am. Chem. Soc.* **1989**, *111*, 165.
(14) (a) Wade, K. J. *J. Chem. Soc. D* **1971**, 792; *Adv. Inorg. Chem. Radiochem.* **1976**, *18*, 1. (b) Mingos, D. M. P. *Nature (London), Phys. Sci.* **1972**, *236*, 99. (c) Mason, R.; Mingos, D. M. P. *MTP Int. Rev. Sci.: Phys. Chem., Ser. Two* **1975**, *11*, 121. (d) Lauher, J. W. *J. Am. Chem. Soc.* **1978**, *100*, 5305. (e) Teo, B. K. *Inorg. Chem.* **1984**, *23*, 1251.
(15) Housecroft, C. E.; O'Neill, M. E.; Wade, K.; Smith, B. C. *J. Organomet. Chem.* **1981**, *213*, 35.
(16) Martinengo, S.; Giordano, G.; Chini, P.; *Inorg. Synth.* **1980**, *20*, 209.

Table II. Relevant Bond Angles (deg) in the Dianion $[PtRh_6(CO)_{16}]^{2-}$

M–M–M			
Rh(1)–Pt–Rh(2)	57.03 (6)	Rh(1)–Rh(5)–Rh(3)	90.97 (8)
Rh(1)–Pt–Rh(6)	62.07 (7)	Rh(1)–Rh(6)–Rh(3)	87.85 (8)
Rh(2)–Pt–Rh(6)	57.05 (7)	Rh(2)–Rh(1)–Rh(4)	90.50 (8)
Pt–Rh(1)–Rh(2)	69.86 (7)	Rh(2)–Rh(3)–Rh(4)	92.78 (9)
Pt–Rh(1)–Rh(6)	60.24 (6)	Rh(2)–Rh(5)–Rh(4)	91.02 (8)
Pt–Rh(2)–Rh(1)	53.11 (6)	Rh(2)–Rh(6)–Rh(4)	91.03 (9)
Pt–Rh(2)–Rh(6)	54.48 (6)	Rh(5)–Rh(1)–Rh(6)	90.30 (8)
Pt–Rh(6)–Rh(1)	57.69 (6)	Rh(5)–Rh(3)–Rh(6)	90.87 (8)
Pt–Rh(6)–Rh(2)	68.47 (7)	Rh(5)–Rh(2)–Rh(6)	87.73 (8)
Rh(1)–Rh(2)–Rh(3)	87.73 (8)	Rh(5)–Rh(4)–Rh(6)	90.20 (9)
Rh(1)–Rh(4)–Rh(3)	88.91 (9)		
M–C–O (Terminal)			
Pt–C(8)–O(8)	179 (3)	Rh(3)–C(3)–O(3)	175 (3)
Rh(1)–C(1)–O(1)	178 (2)	Rh(4)–C(4)–O(4)	174 (3)
Rh(2)–C(2)–O(2)	158 (3)	Rh(5)–C(5)–O(5)	176 (3)
Rh(2)–C(7)–O(7)	173 (2)	Rh(6)–C(6)–O(6)	173 (2)
M–C–M and M–C–O (Double Bridge)			
Pt–C_b(1)–Rh(1)	81.7 (11)	Rh(3)–C_b(2)–O(2)	134 (2)
Pt–C_b(5)–Rh(6)	85.2 (11)	Rh(5)–C_b(2)–O(2)	142 (2)
Rh(3)–C_b(2)–Rh(5)	84.7 (11)	Rh(3)–C_b(3)–O(3)	137 (2)
Rh(3)–C_b(3)–Rh(4)	85.3 (11)	Rh(4)–C_b(3)–O(3)	137 (2)
Rh(4)–C_b(4)–Rh(5)	88.8 (12)	Rh(4)–C_b(4)–O(4)	134 (2)
Pt–C_b(1)–O(1)	134 (2)	Rh(5)–C_b(4)–O(4)	137 (2)
Pt–C_b(5)–O(5)	130 (2)	Rh(6)–C_b(5)–O(5)	144 (3)
Rh(1)–C_b(1)–O(1)	144 (2)		
M–C–M and M–C–O (Triple Bridge)			
Rh(1)–C_t(1)–Rh(4)	80.4 (9)	Rh(1)–C_t(1)–O(1)	134 (2)
Rh(1)–C_t(1)–Rh(6)	82.2 (9)	Rh(4)–C_t(1)–O(1)	126 (2)
Rh(4)–C_t(1)–Rh(6)	78.4 (8)	Rh(6)–C_t(1)–O(1)	135 (2)
Rh(1)–C_t(2)–Rh(5)	73.8 (9)	Rh(1)–C_t(2)–O(2)	130 (2)
Rh(1)–C_t(2)–Rh(2)	80.0 (10)	Rh(2)–C_t(2)–O(2)	134 (2)
Rh(2)–C_t(2)–Rh(5)	80.4 (10)	Rh(5)–C_t(2)–O(2)	136 (2)
Rh(2)–C_t(3)–Rh(3)	75.5 (9)	Rh(2)–C_t(3)–O(3)	130 (2)
Rh(2)–C_t(3)–Rh(6)	82.6 (10)	Rh(3)–C_t(3)–O(3)	127 (2)
Rh(3)–C_t(3)–Rh(6)	80.2 (9)	Rh(6)–C_t(3)–O(3)	139 (2)

uum-dried; the residue was treated under nitrogen with a solution of $Na[PtRh_5(CO)_{15}]$ (378 mg, 0.328 mmol) in 7 mL of methanol. The mixture was stirred for 3 h, yielding a green solution. Addition of $[PPh_4]Br$ (550 mg in 5 mL of 2-propanol) gave a precipitation of green flakes, and further addition of 2-propanol (10 mL) completed the precipitation. The product was filtered, washed with 2-propanol (10 mL), with water (10 mL), then again with 2-propanol (10 mL), and dried under vacuum. This crude product was extracted with 10 mL of THF to give a green solution from which, by slow diffusion of 2-propanol (30 mL), black crystals of the product were obtained.

Crystals of $[N\text{-}n\text{-}Pr_4]_2[PtRh_6(CO)_{16}]$ suitable for X-ray diffraction studies were obtained similarly with use of $[N\text{-}n\text{-}Pr_4]Br$.

(d) By Reduction of $[PtRh_5(CO)_{15}]^-$ under N_2. $Na[PtRh_5(CO)_{15}]$ (273 mg, 0.237 mmol), excess Na_2CO_3 (0.5 g), and methanol (7 mL) were stirred under N_2 with continuous IR monitoring. After a period of 10–15 h, the IR spectrum showed no more starting material and new broad bands around 2000 and 1790 cm^{-1}; the higher yields were obtained by stopping the reaction as soon as this band pattern appeared. This was achieved by filtration of the reaction mixture over Na_2CO_3; the residue, before being discarded, was washed with methanol (5 mL). The solution and collected washings, treated with [PPN]Cl (1.5 g in 6 mL of 2-propanol), gave a partial precipitation, which was completed on further addition of 2-propanol (10 mL). The brown product was filtered, washed with 2-propanol (10 mL), with water (10 mL), and again with 2-propanol (10 mL), and vacuum-dried. Extraction with THF (6 mL) gave a green solution, leaving some oily black residue. Layering of 2-propanol (20 mL) over the THF extract yielded, when the diffusion of the solvents was complete (about 1 week), good-quality black crystals of $[PPN]_2[PtRh_6(CO)_{16}]$ together with a finely powdered material mostly insoluble in THF.

2. X-ray Analysis. A regular prismatic crystal of $[N\text{-}n\text{-}Pr_4]_2[PtRh_6(CO)_{16}]$, with approximate dimensions 0.20 × 0.15 × 0.20 mm, was sealed under N_2 in a capillary for the data collection. The space group and cell constants were determined on the basis of 2θ values of 25 accurately centered high-order reflections on a Phillips PW1100 diffractometer, which was then used for the data collection. The intensities of two standard reflections, measured every 2 h to check the stability and orientation of the crystal, showed no significant variations. Data were corrected for Lorentz and polarization factors, and an empirical absorption correction was applied with use of azimuthal ψ scans. Crystallographic data are listed in Table III.

Table III. Crystallographic Data for $[N\text{-}n\text{-}Pr_4]_2[PtRh_6(CO)_{16}]$

chem formula: $C_{40}H_{56}N_2O_{16}PtRh_6$	fw = 1633.41
a = 17.180 (2) Å	space group: $C2/c$ (No. 15)
b = 15.848 (2) Å	T = room temp
c = 39.719 (4) Å	λ = 0.710 69 Å
β = 92.45 (3)°	ρ_{calcd} = 2.01 g cm^{-3}
V = 10 804 (4) Å^3	μ = 44.3 cm^{-1}
Z = 8	transmission coeff: 0.56–0.78
$R(F_o)$ = 0.048	$R_w(F_o)$ = 0.063

Table IV. Atomic Coordinates for the Anion of $[N\text{-}n\text{-}Pr_4]_2[PtRh_6(CO)_{16}]$[a]

atom	x/a	y/b	z/c
Pt	0.10670 (7)	0.51298 (9)	0.17581 (3)
Rh(1)	0.26308 (11)	0.51277 (14)	0.17185 (5)
Rh(2)	0.19163 (12)	0.46304 (13)	0.10946 (5)
Rh(3)	0.26839 (12)	0.59885 (14)	0.07977 (5)
Rh(4)	0.33343 (12)	0.65223 (14)	0.14043 (5)
Rh(5)	0.35532 (11)	0.48723 (14)	0.11784 (5)
Rh(6)	0.17278 (11)	0.63081 (14)	0.13411 (5)
C(1)	0.3559 (15)	0.4976 (18)	0.1960 (7)
O(1)	0.4155 (13)	0.4881 (15)	0.2125 (6)
C(2)	0.0997 (19)	0.4087 (21)	0.1213 (8)
O(2)	0.0498 (14)	0.3549 (16)	0.1208 (6)
C(3)	0.2481 (19)	0.6328 (21)	0.0366 (8)
O(3)	0.2394 (13)	0.6519 (15)	0.0074 (6)
C(4)	0.3813 (18)	0.7482 (20)	0.1624 (8)
O(4)	0.4097 (15)	0.8072 (17)	0.1726 (6)
C(5)	0.4302 (16)	0.4033 (19)	0.1197 (7)
O(5)	0.4810 (14)	0.3538 (16)	0.1213 (6)
C(6)	0.1694 (15)	0.7457 (17)	0.1247 (7)
O(6)	0.1657 (12)	0.8198 (14)	0.1201 (5)
C(7)	0.2098 (16)	0.4147 (18)	0.0667 (7)
O(7)	0.2125 (15)	0.3862 (14)	0.0400 (5)
C(8)	0.0245 (19)	0.4803 (22)	0.1979 (9)
O(8)	−0.0307 (12)	0.4586 (13)	0.2133 (5)
C_b(1)	0.1993 (17)	0.4547 (19)	0.2051 (8)
O_b(1)	0.2017 (12)	0.4084 (14)	0.2275 (5)
C_b(2)	0.3606 (16)	0.5221 (18)	0.0696 (7)
O_b(2)	0.3944 (10)	0.5068 (12)	0.0445 (5)
C_b(3)	0.3350 (15)	0.7009 (18)	0.0939 (7)
O_b(3)	0.3597 (12)	0.7640 (13)	0.0808 (5)
C_b(4)	0.4266 (17)	0.5821 (19)	0.1329 (7)
O_b(4)	0.4953 (12)	0.5918 (13)	0.1386 (5)
C_b(5)	0.0653 (17)	0.6213 (19)	0.1495 (8)
O_b(5)	0.0040 (14)	0.6517 (15)	0.1480 (6)
C_t(1)	0.2434 (14)	0.6447 (16)	0.1798 (6)
O_t(1)	0.2403 (11)	0.6898 (12)	0.2053 (5)
C_t(2)	0.2708 (16)	0.3926 (19)	0.1401 (7)
O_t(2)	0.2740 (10)	0.3192 (12)	0.1489 (5)
C_t(3)	0.1368 (16)	0.5836 (18)	0.0882 (7)
O_t(3)	0.0854 (11)	0.5923 (12)	0.0684 (5)

[a] Coordinates of the atoms in the cations are given as supplementary material.

The structure was solved by standard Patterson and Fourier techniques and refined by block-diagonal least squares with anisotropic thermal factors for the Pt and Rh atoms. The function minimized was $[\sum w(|F_o| - 1/k|F_c|)^2]^{1/2}$ by using a Cruickshank[17] weighting scheme. Scattering factors were taken from ref 18. The correction for the real part of the anomalous dispersion[18] was taken into account for the Pt and Rh atoms. Upon convergence, the final Fourier difference map showed no unusual features. Final atomic coordinates are reported in Table IV.

Supplementary Material Available: Tables of crystallographic data and collection parameters (Table S1), thermal parameters (Table S2), and positional parameters of the cations (3 pages); a list of observed (F_o) and calculated (F_c) structure factors (Table S3) (26 pages). Ordering information is given on any current masthead page.

(17) Cruickshank, D. W. J. *Computing Methods in Crystallography*; Ahmed, A., Ed.; Munksgaard: Copenhagen: 1972.
(18) *International Tables for X-ray Crystallography*; Kynoch Press: Birmingham, England, 1974; Vol. IV.